Half-metallic electronic structures of giant magnetoresistive spinels: $Fe_{1-x}Cu_xCr_2S_4$ ($x=0.0,0.5,1.0$)

Min Sik Park, S. K. Kwon, S. J. Youn,* and B. I. Min
Department of Physics, Pohang University of Science and Technology, Pohang 790-784, Korea
(Received 18 November 1998)

Electronic structures of Cr-based chalcogenide spinels $Fe_{1-x}Cu_xCr_2S_4$ ($x=0.0,0.5,1.0$) are investigated by using the linearized muffin-tin orbital (LMTO) band method in both the local-spin-density approximation (LSDA) and the LSDA+U. The LSDA yields the half-metallic electronic structures for $x=0.0,1.0$ and the insulating electronic structure for $x=0.5$. The LSDA+U yields the insulating electronic structures for $x=0.0$ in agreement with experiments. The orbital ordering driven by the on-site Coulomb interaction for $x=0.0$ is demonstrated based on the LSDA+U electronic structures. Orbital magnetic moment M_{orb} is obtained by taking into account the spin-orbit interaction. M_{orb}'s of Fe and Cu in these compounds are found to be very large, reflecting the localized features of $3d$ band electrons. Conduction models for $x=0.0,0.5,1.0$ are discussed with the schematic energy diagrams incorporating the Jahn-Teller effect and the half-metallic electronic structures. [S0163-1829(99)15515-2]

I. INTRODUCTION

Recently discovered colossal magnetoresistance (CMR) phenomena have attracted considerable attention, because of the potential for technological applications and the intriguing physical properties of materials.[1] The CMR phenomena are observed in cubic perovskite manganites $R_{1-x}A_xMnO_3$ (R = rare earth; A = divalent cation), layered manganites $(LaSr)_3Mn_2O_7$,[2] and $Tl_2Mn_2O_7$ with pyrochlore structure.[3,4]

Albeit not so colossal, very large negative magnetoresistance has been observed also in Cr-based chalcogenide $Fe_{1-x}Cu_xCr_2S_4$ ($x=0.0,0.5$) with spinel structure.[5] Figure 1 shows the magnetization M, the resistivity ρ, and the magnetoresistance (MR) as a function of temperature for $Fe_{1-x}Cu_xCr_2S_4$ ($x=0.0$ and 0.5). Under the magnetic field of 6 T, the MR for $x=0.0$ amounts to $\sim$20% near the magnetic transition temperature $T_c=170$ K, and for $x=0.5$, $\sim$7% near $T_c=340$ K. As compared to $\sim$100% MR of perovskite manganites, the MR of Cr-based chalcogenides is relatively small. Still this size of MR is as large as in giant magnetoresistance (GMR) metallic multilayers. As in perovskite manganites, the metal-insulator transition seems to occur simultaneously with the magnetic phase transition, and the peak position of the MR curve coincides with T_c. The magnetic phase in this case is ferrimagnetic, Fe and Cr spins polarize antiferromagnetically. The resistivities ρ in both cases ($x=0.0$ and 0.5) manifest semiconducting behaviors $[(d\rho/dT)<0]$ for $T>T_c$ and $T\ll T_c$, while, in the finite-temperature range below T_c, metallic features are observed. The temperature range showing the metallic feature is wider for $x=0.5$.

In fact, the large negative magnetoresistance phenomena in the spinel $Fe_{1-x}Cu_xCr_2S_4$ have been already reported.[6] The observed MR with the external magnetic field of 1.3 T was $\sim$6% for $x=0.0$. Furthermore, the question on the Cu valence state in $CuCr_2S_4$ has been the longstanding

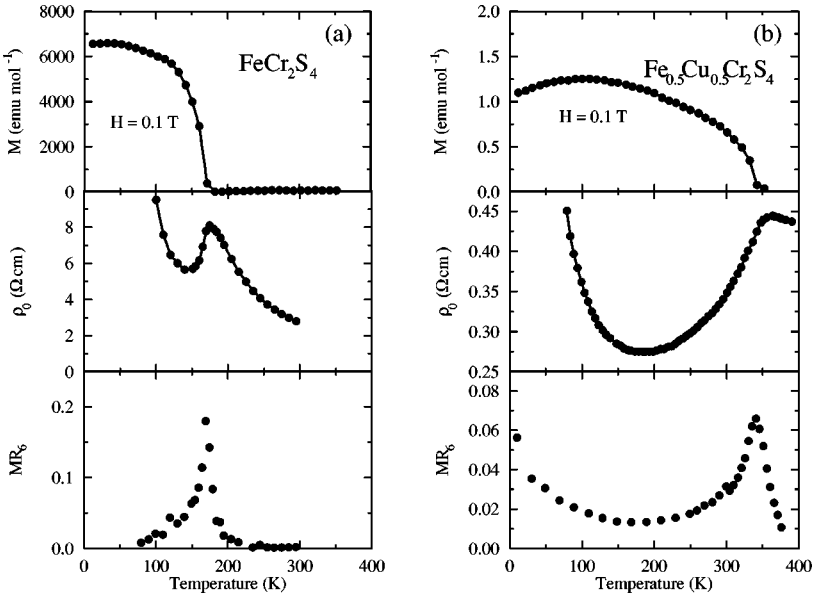

FIG. 1. Magnetization (M), resistivity (ρ), and magnetoresistance ($MR_H=\{[\rho(0)-\rho(H)]/\rho(0)\}$) vs temperature for $FeCr_2S_4$ (left), $Fe_{0.5}Cu_{0.5}Cr_2S_4$ (right). (Adapted from Ref. 5.)

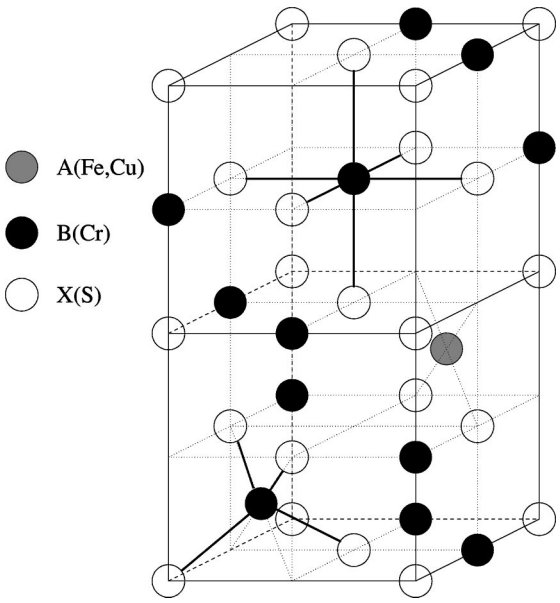

FIG. 2. Spinel structure AB_2X_4; A,B ions are at tetrahedral and octahedral sites, respectively.

problem.[7,8] Lotgering[7] claimed that the Cu valence state should be monovalent, while Goodenough[8] claimed that it should be divalent. Various experiments give different results on the Cu valence state. The electronic structure of $CuCr_2S_4$ was once calculated by Horikawa *et al.*[9] by using the discrete variational (DV)-X_α method based on the Hartree-Fock-Slater model.[10] They obtained the half-metallic electronic structure for $CuCr_2S_4$, even though they did not use such a terminology. In the half-metal, the charge carriers are fully polarized: the one spin band is metallic whereas the other spin band is insulating.[11,12]

In this study, we have investigated electronic structures of Cr-based chalcogenide $Fe_{1-x}Cu_xCr_2S_4$ ($x=0.0,0.5,1.0$) by using both the local-spin-density approximation (LSDA) and the LSDA+U (LSDA incorporating the on-site Coulomb interaction U) method[13] on the basis of the linearized muffin-tin orbital (LMTO) band method. The von Barth–Hedin form of the exchange-correlation potential is utilized, and 40 $\vec{k}$ points inside the irreducible Brillouin zone are used for the integration. It is found that the LSDA yields half-metallic electronic structures for $Fe_{1-x}Cu_xCr_2S_4$ ($x=0.0,1.0$) and the insulating electronic structure for $x=0.5$. The ground state insulating nature of $x=0.0$ can be described well by the LSDA+U method. The orbital contribution to the magnetic moment is examined by including the spin-orbit interaction in a perturbative way.[14] Both the magnetic exchange-correlation interaction and the spin-orbit interaction are taken into account simultaneously in the self-consistent step. Transport properties of this compound are explored based on the half-metallic electronic structure. Further, physical properties of the Jahn-Teller effect and the orbital ordering induced by the on-site Coulomb interaction are discussed.

II. CRYSTAL STRUCTURE AND THE JAHN-TELLER EFFECT

$FeCr_2S_4$ and $CuCr_2S_4$ crystallize in the spinel structure AB_2X_4 (see Fig. 2). The ideal spinel structure is formed by a cubic close-packed (fcc) array of X atoms, in which one-eighth of the tetrahedral and one-half of the octahedral interstitial sites are occupied by cations. The tetrahedrally coordinated sites and the octahedrally coordinated sites are referred to as A and B sites, respectively. The X atoms have fourfold coordination, formed by three B cations and one A cation. There are two formula units in the primitive unit cell, and for the LMTO calculation, four empty spheres are considered in the interstitial sites to enhance the packing ratio.

TABLE I. Spin magnetic moments in μ_B of spinel $Fe_{1-x}Cu_xCr_2S_4$ from the LSDA+U calculation at the experimental lattice constant. Total in the table corresponds to the total spin magnetic moment per formula unit, and *ES* denotes the empty sphere.

	Total	Cr	Fe	Cu	S	ES
$x=0.0$	2.00	3.11	−3.70		−0.11	−0.05
$x=0.5$	3.50	3.11	−3.95	−0.30	−0.14	−0.01
$x=1.0$	5.00	3.04		−0.50	−0.15	−0.00

In the spinel structure, five degenerate d levels of transition metals, A and B, are split into two levels by the crystal field, caused by the electrostatic interaction between d orbitals of cations and p orbitals of nearby anions.[15] One is the triplet (t_{2g}) which consists of d_{xy}, d_{yz}, and d_{zx} levels, and the other is the doublet (e_g) which consists of $d_{3z^2-r^2}$ and $d_{x^2-y^2}$ levels. The energy difference between two levels is labeled by $10Dq$. In the octahedral sites, energy levels of t_{2g} are lower than energy levels of e_g, whereas, in the tetrahedral sites, the situation is reversed.

When these t_{2g} and e_g levels are not fully occupied, the Jahn-Teller instability can occur. Then the degenerate energy level is split further again by reducing the crystal symmetry. Accordingly, the lattice distortion is induced by the Jahn-Teller instability.[16] In the case of $Fe_{1-x}Cu_xCr_2S_4$, both Fe and Cu are expected to behave as Jahn-Teller active ions, if their valence states are $Fe^{2+}(d^6)$ and $Cu^{2+}(d^9)$.

III. RESULTS AND DISCUSSION

A. $FeCr_2S_4$ ($x=0.0$)

The LSDA electronic structure calculation yields the ferrimagnetic half-metallic state for $FeCr_2S_4$ at the experimental lattice constant $a=9.989$ Å. Spins of Fe and Cr ions polarize antiferromagnetically. The metallic nature from the LSDA, however, does not seem to agree with the experiment showing that the ground state of $FeCr_2S_4$ would be insulating [Fig. 1(a)]. Therefore, one has to invoke some other mechanism to have an insulating ground state. One possible mechanism is the Jahn-Teller effect. Obtained results of magnetic moments in Table I are in good agreement with the experiments,[17] which suggests that $FeCr_2S_4$ has a normal spinel valence configuration such that $Fe^{2+}Cr_2^{3+}S_4^{2-}$. Since Fe^{2+} with d^6 electrons is a Jahn-Teller active ion in the tetrahedral interstitial sites, it is expected that the energy splitting will occur due to the Jahn-Teller effect at Fe sites to result in the insulating ground state. Indeed, Spender and Morrish[18] have found that the tetrahedral site of $FeCr_2S_4$ is distorted below $T=10$ K by the Jahn-Teller effect exhibit-

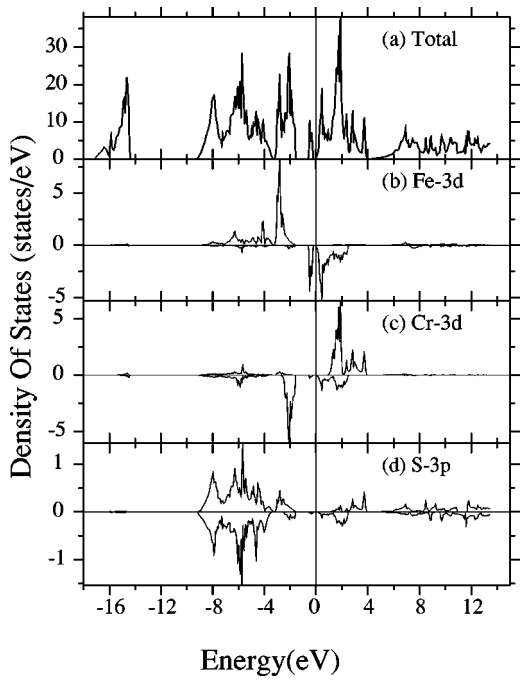

FIG. 3. Total and projected local density of states (PLDOS) from the LSDA+U calculation for $FeCr_2S_4$. Parameters used are $U=2.5, J=0.94$ eV for Fe and $U=1.5, J=0.89$ eV for Cr. (a) Total DOS per unit cell (two formula units), (b) PLDOS of Fe-3d, (c) PLDOS of Cr-3d, (d) PLDOS of S-3p.

ing the tetragonal structure. Hence, once taking into account the Jahn-Teller distortion in the calculations, the LSDA is expected to yield a correct insulating ground state for $FeCr_2S_4$.

Another possible mechanism to produce an insulating ground state for $FeCr_2S_4$ is the Coulomb correlation effect. Since d electrons at Fe and Cr sites of $FeCr_2S_4$ are rather localized, the LSDA may not describe properly their correlated natures. This is related to the well-known band gap problem of the local density approximation (LDA), as also seen in the wrong LDA prediction of a metallic phase for undoped high-Tc cuprates. The correlation effect can be taken into account in a mean field way by the LSDA+U method incorporating the on-site inter-d-orbital Coulomb interaction U.[13] The LSDA+U method gives rise to the correct insulating ground state for $FeCr_2S_4$ (see Fig. 3). We have used U values of 2.5 and 1.5 eV for Fe and Cr, respectively. These U values are somewhat smaller than those used in LSDA+U calculations for transition metal oxides.[13] The first-principles determination of the U parameter is still lacking, but it is expected that the U values in metallic transition metals or in intermetallic transition metal compounds are smaller than in transition metal oxides.[19,20] Hence we have chosen here rather smaller values of U, which are comparable to those for intermetallic transition metal compounds, to see the Coulomb correlation effect on the band structure. The Hund's coupling exchange parameter J is also employed in the LSDA+U calculation, 0.94 and 0.89 eV for Fe and Cr, respectively. It is seen in Fig. 3 that the extra Coulomb interaction between d orbitals induces the energy splitting to manifest a small energy gap in the density of states (DOS) near the Fermi level (E_F).

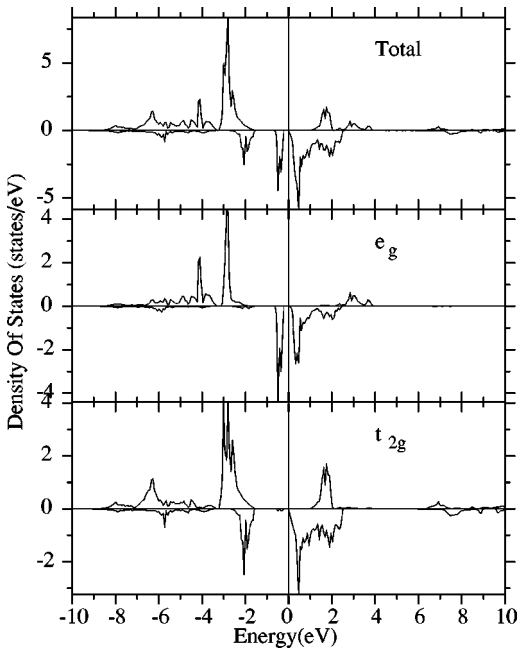

FIG. 4. Partial e_g and t_{2g} PLDOS of Fe in $FeCr_2S_4$.

The structures in the DOS near E_F originate mainly from the minority spin band of Fe-3d electrons. Thus, due to the Coulomb interaction, the minority spin e_g band of Fe is split into two subbands, and only the lower subband is occupied. The local density of states (LDOS) in Fig. 4 shows that the occupied one has a predominant $d_{3y^2-r^2}$ character, while the empty one a $d_{z^2-x^2}$ character. This splitting produces the orbital ordering of d orbitals. Figure 5 provides the minority spin density of e_g electrons at Fe sites, which clearly indicates that the orbital ordering with dominant $d_{3y^2-r^2}$ character occurs due to the Coulomb interaction. Such an orbital ordering will in turn drive the lattice distortion in the tetrahedral Fe sites, which will reproduce the experimentally observed cooperative Jahn-Teller effect.

The orbital contribution to the magnetic moment is obtained by incorporating the spin-orbit interaction in the self-consistent band calculation. The orbital magnetic moment M_{orb} in $FeCr_2S_4$ turns out to be substantial. The total M_{orb} per formula unit amounts to $-0.31\mu_B$, most of which comes from Fe ion which has $-0.24\mu_B$. This is very large as compared to M_{orb} of the bcc Fe$\sim 0.03\mu_B$. Such a large M_{orb} of Fe in $FeCr_2S_4$ implies that the Fe-3d electrons in $FeCr_2S_4$ are very localized as compared to those in bcc Fe.

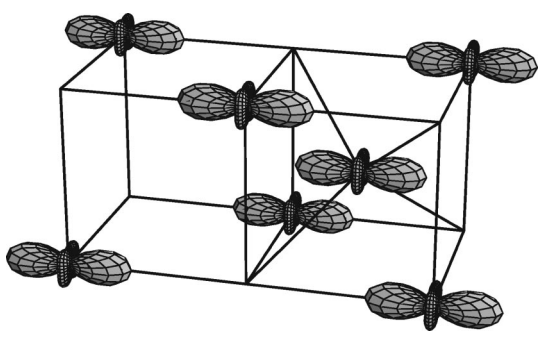

FIG. 5. The calculated angular distribution (orbital ordering) of the minority spin density of Fe e_g band in $FeCr_2S_4$.

Now, let us examine the temperature dependent resistivity behavior of $FeCr_2S_4$. Figure 1(a) indicates that $FeCr_2S_4$ possesses an insulating nature in most of the temperature range except for $T=150-180$ K. With increasing the temperature, the insulator-metal transition occurs at $T\sim150$ K, and the metal-insulator transition occurs again at $T\sim180$ K. The insulating nature below $T=140$ K can be understood by the Jahn-Teller and the Coulomb correlation effect, as mentioned above. The origin of metallic nature for $T=150-180$ K is rather uncertain. The double exchange interaction operating in the perovskite manganites will not play a role here, since no mixed-valent cations are expected in $FeCr_2S_4$.[21] Nevertheless, it is interesting to note that the overall behavior of temperature dependent resistivity of $FeCr_2S_4$ is quite similar to that of doped manganite $La_{0.85}Sr_{0.15}MnO_3$.[22] The resistivity behavior in $La_{0.85}Sr_{0.15}MnO_3$ is qualitatively understood using the small polaron model. That is, the insulator to metal transition at high temperature corresponds to the thermal to band hopping transition of the small polarons,[23] while the metal to insulator transition at low temperature corresponds to the polaron ordering transition.[24]

In $FeCr_2S_4$, it was suggested that the static Jahn-Teller distortion transforms into the dynamic one near $T=10$ K.[18] Thus, one can expect that small polarons are formed in $FeCr_2S_4$ by the dynamical Jahn-Teller phonon-electron interaction. Observed anomalies in the phonon frequency and the damping constant near T_c corroborates the strong electron-phonon interaction in this system.[25] In this scheme, one can explain the insulator to metal transition near $T=150$ K in terms of the suppression of the Jahn-Teller instability and the concomitant disappearance of the energy gap. The metal to insulator transition at $T_c=180$ K can be understood by considering the band to thermal hopping transition of the small polarons, and so the insulating behavior above T_c originates from the thermal hopping of small polarons, as in perovskite manganites.[23,26]

One can anticipate that, in the temperature range of $T=150-180$ K, metallic $FeCr_2S_4$ has a half-metallic electronic structure, as the LSDA predicts. With increasing the temperature toward T_c, the energy gap induced by the Jahn-Teller effect and the on-site Coulomb interaction vanishes, and so the LSDA results are expected to be effective. The large negative MR is closely related to the half-metallic nature, because the conduction becomes much more enhanced by aligning the magnetic domains through the external magnetic field. In half-metallic systems, there is no Stoner continuum to which charge carriers can transit with flipping their spins. Hence the spin-flip scattering is suppressed, and so the resistivity will decrease with applying the magnetic field. Moreover, half-metallic property can increase MR by contributing tunneling between magnetic grains. The MR due to tunneling between ferromagnetically coupled grains is proportional to the polarization of the tunneling electrons. In half-metallic ferromagnets, electrons near E_F are fully spin polarized, and so the MR can be larger than in normal ferromagnetic metals.[27]

This can be easily understood from the schematic energy diagram of Fig. 6, which is drawn based on the half-metallic LDOS (Fig. 4) with the valence configuration $Fe^{2+}Cr_2^{3+}S_4^{2-}$. The LDOS of Fig. 4 indicates that the exchange splittings $\Delta_{ex}(=SJ)$ at Fe and Cr sites are larger than the crystal field splittings ($\Delta_{ex}\sim3-4$ eV:$10Dq\sim1$ eV). Hence the spin configurations at both ions are high spin states, that is, the spin-up bands (e_g and t_{2g}) at Fe are fully occupied, and the spin-down t_{2g} band at Cr is also fully occupied. The conduction electrons are mainly from the spin-down e_g band of Fe. Therefore, one can expect the spin-polarized tunneling of e_g electrons of Fe becomes much more effective with all the magnetic domains aligned, and so the MR ratio is expected to become very large.

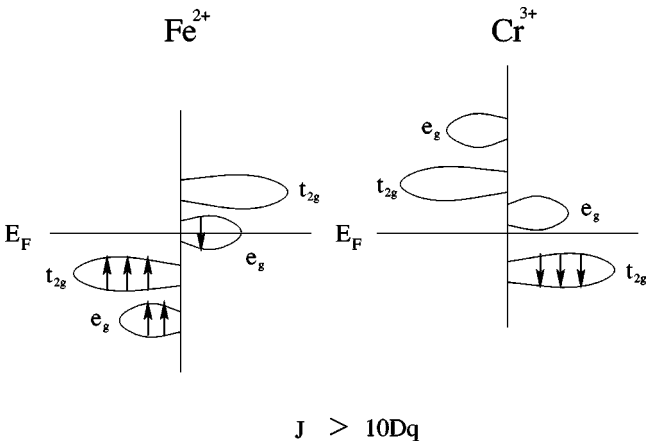

FIG. 6. Schematic energy diagram of half-metallic $FeCr_2S_4$. Note that $FeCr_2S_4$ has an insulating ground state.

On the other hand, one has to pay attention to other possible mechanisms. There have been several approaches to understand the transport phenomena in ferromagnetic semiconductors such as $FeCr_2S_4$, $CdCr_2Se_4$, and EuO. Haacke and Beegle[28] proposed that the magnon-hole interaction is responsible for the anomalous thermopower of $FeCr_2S_4$ near T_c. Kogan and Auslender[29] proposed the Anderson localization due to spin disorder to explain the resistivity peak observed in In doped $CdCr_2Se_4$. The T-dependent resistivity of doped $CdCr_2Se_4$ is very similar to that of $FeCr_2S_4$. The conducting carriers in doped $CdCr_2Se_4$ are produced by In doping. As compared to $FeCr_2S_4$, there are no Jahn-Teller active ions in $CdCr_2Se_4$. Rather, there might exist some contribution of the double exchange interaction due to possible mixed-valent Cr ions in doped $CdCr_2Se_4$. So the origin of the resistivity peak in doped $CdCr_2Se_4$ may not be the same as in $FeCr_2S_4$. Further theoretical and experimental studies are necessary to identify the conduction mechanisms in these spinel ferromagnetic semiconductors.

B. $CuCr_2S_4$ ($x=1.0$)

For $CuCr_2S_4$ at the experimental lattice constant $a=9.814$ Å, both the LSDA and LSDA+U calculations yield the ferromagnetic half-metallic ground state, which is consistent with the experiment (see Fig. 7). In LSDA+U calculations, parameters $U=2.5$, $J=0.89$ eV for Cu and $U=1.5$, $J=0.89$ eV for Cr are used. The LDOS of Cr in the octahedral sites of $CuCr_2S_4$ is similar to that of Cr in $FeCr_2S_4$. This means that the condition $J>10Dq$ is also satisfied for Cr ions in $CuCr_2S_4$, and so the schematic energy diagram at Cr is as in Fig. 8 to have a high spin state. On the other hand, the condition of $J>10Dq$ is not satisfied for Cu

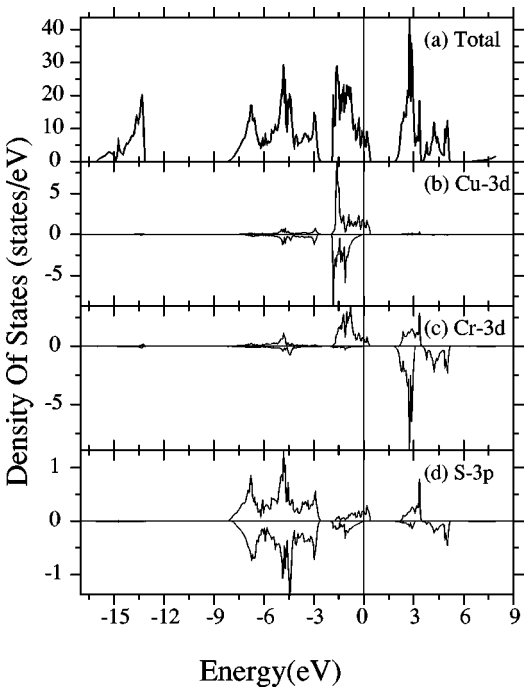

FIG. 7. Total and projected local DOS from the LSDA+U calculation for $CuCr_2S_4$. Parameters used are $U=2.5, J=0.89$ eV for Cu and $U=1.5, J=0.89$ eV for Cr. (a) Total DOS per unit cell (two formula units), (b) PLDOS of Cu-3d, (c) PLDOS of Cr-3d, (d) PLDOS of S-3p.

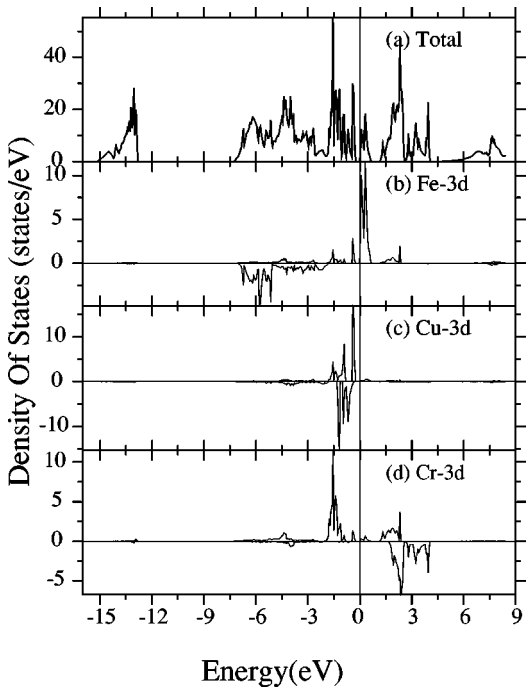

FIG. 9. Total and projected local DOS from the LSDA+U calculation for $Fe_{0.5}Cu_{0.5}Cr_2S_4$. Parameters used are $U=2.5, J=0.94$ eV for Fe, $U=2.5, J=0.89$ eV for Cu, and $U=1.5, J=0.89$ eV for Cr. (a) Total DOS per unit cell (two formula units), (b) PLDOS of Fe-3d, (c) PLDOS of Cu-3d, (d) PLDOS of Cr-3d.

ions, and so the Cu ion has a low spin state, and contributes charge carriers (hole or electron) to show a metallic behavior in $CuCr_2S_4$. From this, one can expect that the spins of mobile carriers are fully polarized.

The calculated spin magnetic moment $5\mu_B$ (Table I) is consistent with the value as described by Goodenough.[8,15] He explained that this value comes from two Cr ions having a local magnetic moment of $3\mu_B$ and the antiparallel spin-polarization of the antibonding σ^* band having $-1\mu_B$. The spin density of σ^* band is not localized only at Cu sites but spread over the crystal. Experimental results[30] also support this idea. This result reflects that $CuCr_2S_4$ has a normal spinel valence configuration $Cu^{2+}Cr_2^{3+}S_4^{2-}$, even though the bonding nature is not fully accounted for by the ionic model.

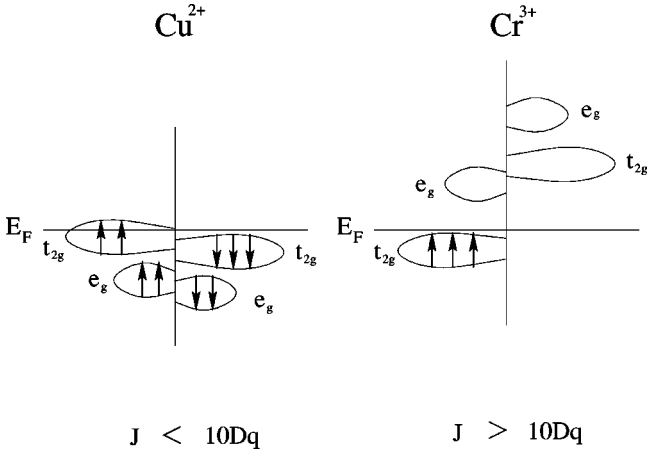

FIG. 8. Schematic energy diagram of half-metallic $CuCr_2S_4$.

Since the Cu^{2+} with d^9 electronic configuration in the tetrahedral interstitial sites is Jahn-Teller active, it is possible to have the Jahn-Teller effect in $CuCr_2S_4$. However, so far, the Jahn-Teller distortion is not observed in the experiment.[30]

The orbital magnetic moment M_{orb} in $CuCr_2S_4$ is also very large. The total M_{orb} per formula unit amounts to $-0.15\mu_B$, and the M_{orb} of Cu ion corresponds to $-0.09\mu_B$. This again indicates that the Cu-3d electrons in $CuCr_2S_4$ are still localized, and the 3d band of Cu is not fully occupied.

Note, however, that other valence configurations were also proposed, such as $Cu^+[Cr^{3+}Cr^{4+}]Se_4^{2-}$ with monovalent Cu[7] or $Cu^+_{1-n}Cu^{2+}_n[Cr^{3+}_{1+n}Cr^{4+}_{1-n}]X_4^{2-}$ (X=S,Se), which shows temperature-dependent valence configurations.[31] In these cases, there are mixed-valent Cr or Cu ions, and so the ferromagnetic ground state can be explained in terms of the double exchange interaction.[32] As yet, there is no experimental agreement on the valence configuration of $CuCr_2S_4$, which remains to be resolved.

C. $Fe_{0.5}Cu_{0.5}Cr_2S_4$ ($x=0.5$)

We have performed the electronic structure calculation for $Fe_{0.5}Cu_{0.5}Cr_2S_4$ by replacing one Fe by Cu in the unit cell of two formula unit $FeCr_2S_4$. For $Fe_{0.5}Cu_{0.5}Cr_2S_4$ for $a=9.904$ Å, both the LSDA and the LSDA+U calculations yields the ferrimagnetic and insulating ground state (Fig. 9), which is consistent with the experiment at low temperature [Fig. 1(b)]. In the LSDA+U calculations, parameters used are $U=2.5$, $J=0.94$ eV for Fe, $U=2.5$, $J=0.89$ eV for Cu, and $U=1.5$, $J=0.89$ eV for Cr. The reason why the LSDA yields the correct insulating ground state for

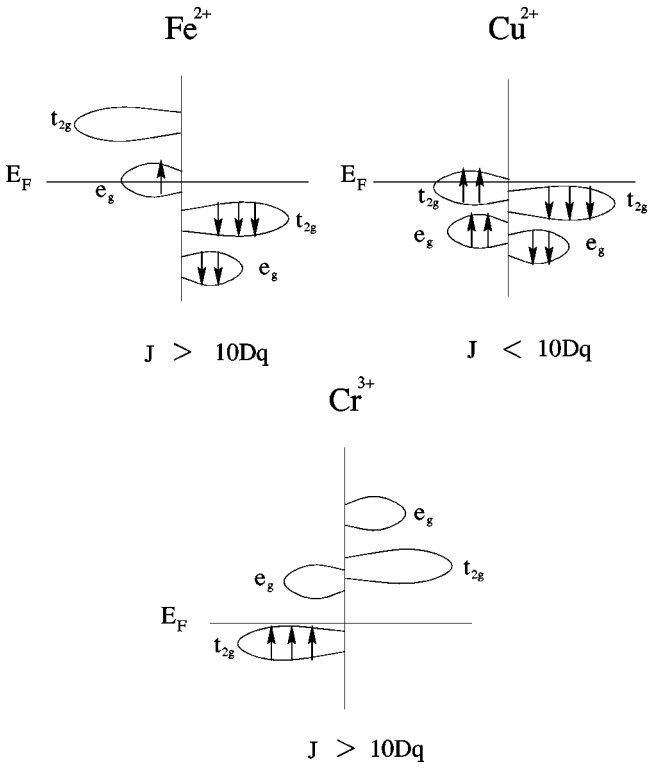

FIG. 10. Schematic energy diagram of $Fe_{0.5}Cu_{0.5}Cr_2S_4$.

$Fe_{0.5}Cu_{0.5}Cr_2S_4$ is that the different ionic potentials of Fe and Cu sites in the unit cell induce the band splitting with a band gap near E_F.

Distinctly from the case of $FeCr_2S_4$, the LSDA+U calculations do not give the definite orbital ordering of d orbitals. This suggests that the d-electrons in $Fe_{0.5}Cu_{0.5}Cr_2S_4$ are not so localized as in $FeCr_2S_4$. This feature is again consistent with the experiment observations. Note in Fig. 9 that the temperature range showing metallic property ($T=180 \sim 360$ K) is much wider in $x=0.5$ than in $x=0.0$, reflecting that the carriers in $x=0.5$ are more delocalized than in $x=0.0$. The delocalized nature of d electrons causes the d band wider, and so the splitting due to the orbital ordering seems to be smeared out. As in $x=0.0$, we expect that $x=0.5$ has a half-metallic electronic structure in the temperature range showing metallic property.

The valence configuration of $x=0.5$ can have two possible cases. The first possibility is a normal spinel configuration, $Fe^{2+}_{0.5}Cu^{2+}_{0.5}Cr^{3+}_2S^{2-}_4$. This configuration is consistent with the calculated magnetic moments (Table I). Then the schematic energy diagram corresponds to Fig. 10. In this case, Fe^{2+} and Cu^{2+} are Jahn-Teller active ions, and so the Jahn-Teller distortion may occur. However, due to more delocalized nature of conduction electrons, the effect is expected to be observed only at very low temperature. The total orbital magnetic moment M_{orb} per formula unit of $Fe^{2+}_{0.5}Cu^{2+}_{0.5}Cr^{3+}_2S^{2-}_4$ amounts to $-0.13\mu_B$, and the M_{orb}'s of Fe and Cu ion correspond to $-0.08\mu_B$ and $-0.06\mu_B$, respectively. This again indicates that the Fe-3d and Cu-3d electrons in $Fe^{2+}_{0.5}Cu^{2+}_{0.5}Cr^{3+}_2S^{2-}_4$ are rather localized, and the 3d band of Cu is not fully occupied. In the case of $Fe^{2+}_{0.5}Cu^{2+}_{0.5}Cr^{3+}_2S^{2-}_4$, the temperature dependent resistivity behavior will be similar to that in the case of $x=0.0$, because of the same valence configuration. In this view, the wider metallic region in $x=0.5$ is due to more delocalized conducting carriers from Cu^{2+}.

The second possible valence configuration is $Fe^{3+}_{0.5}Cu^{1+}_{0.5}Cr^{3+}_2S^{2-}_4$, proposed based on some experimental results.[33–35] In this case, it may be easy to explain the insulating ground state even without the Jahn-Teller and the Coulomb interaction effects. However, this consideration has difficulty in explaining the wide metallic region observed in $x=0.5$.

IV. CONCLUSION

We have studied electronic structures of Cr-based chalcogenide spinels $Fe_{1-x}Cu_xCr_2S_4$ ($x=0.0,0.5,1.0$) by using the LMTO band method in both the LSDA and LSDA+U. We can qualitatively explain the resistivity behavior of $x=0.0,0.5$ based on their half-metallic electronic structures. It is deduced that $Fe_{1-x}Cu_xCr_2S_4$ ($x=0.0,0.5,1.0$) have half-metallic properties in the temperature range showing metallic behaviors, which are expected to have close correlation with observed large negative MR phenomena. The orbital contribution to the magnetic moment obtained by incorporating the spin-orbit interaction turns out to be very large in these compounds, reflecting very localized features of 3d band electrons. The orbital magnetic moments of Fe and Cu are as large as $-0.24\mu_B$ and $-0.09\mu_B$, respectively. Further, we have discussed the Jahn-Teller effects and the orbital orderings, which will be possibly observed in $Fe_{1-x}Cu_xCr_2S_4$. Experiments to measure the orbital magnetic moments and to observe the Jahn-Teller effects at low temperature and the half-metallic property in the metallic regime of $Fe_{1-x}Cu_xCr_2S_4$ are demanded to clarify the origin of such large negative MR phenomena.

ACKNOWLEDGMENTS

We thank J. H. Park and U. J. Yu for helpful discussions. This work was supported by the Korea Research Foundation (Grant No. 1997-001-D00139), and in part by the KOSEF (Grant No. 96-0702-01-01-3).

*Present address: Department of Physics, Northwestern University, Evanston, IL 60208.

[1] S. Jin, T.H. Tiefel, M. McCormack, R.A. Fastnacht, R. Ramesh, and L.H. Chen, Science **264**, 413 (1994).

[2] T. Kimura, A. Asamitsu, Y. Tomioka, and Y. Tokura, Science **274**, 1698 (1996).

[3] Y. Shimakawa, Y. Kubo, and T. Manako, Nature (London) **379**, 53 (1996).

[4] M.A. Subramanian, B.H. Toby, A.P. Ramirez, W.J. Marshall, A.W. Sleight, and G.H. Kwei, Science **273**, 81 (1996).

[5] A.P. Ramirez, R.J. Cava, and J. Krajewski, Nature (London) **386**, 156 (1997).

[6] T. Watanabe and I. Nakada, Jpn. J. Appl. Phys. **17**, 1745 (1978); K. Ando, Y. Nishihara, T. Okuda, and T. Tsushima, J. Appl. Phys. **50**, 1917 (1979).

[7] F.K. Lotgering, Solid State Commun. **2**, 55 (1964).

[8] J.B. Goodenough, Solid State Commun. **5**, 577 (1967).
[9] J.I. Horikawa, T. Hamajima, F. Ogata, T. Kambara, and K.I. Gondaira, J. Phys. C **15**, 2613 (1982).
[10] T. Oguchi, T. Kambara, and K.I. Gondaira, Phys. Rev. B **22**, 872 (1980).
[11] R.A. de Groot, F.M. Mueller, P.G. van Engen, and K.H.J. Buschow, Phys. Rev. Lett. **50**, 2024 (1983).
[12] V.Yu. Irkhin and M.I. Katsnel'son, Usp. Fiz. Nauk **164**, 705 (1994) [Phys. Usp. **37**, 659 (1994)].
[13] V.I. Anisimov, J. Zaanen, and O.K. Andersen, Phys. Rev. B **44**, 943 (1991).
[14] B.I. Min and Y.-R. Jang, J. Phys.: Condens. Matter **3**, 5131 (1991).
[15] J.B. Goodenough, J. Phys. Chem. Solids **30**, 261 (1969).
[16] Raul Valenzuela, *Magnetic Ceramics* (Cambridge University Press, New York, 1994).
[17] G. Haacke and L.C. Beegle, J. Phys. Chem. Solids **28**, 1699 (1967).
[18] M.R. Spender and A.H. Morrish, Solid State Commun. **11**, 1417 (1972).
[19] G. Treglia, F. Ducastelle, and D. Spanjaard, J. Phys. F **43**, 341 (1982).
[20] J.-S. Kang, J.H. Hong, D.W. Hwang, J.I. Jeong, S.D. Choi, C.J. Yang, Y.P. Lee, C.G. Olson, Kicheon Kang, and B.I. Min, Phys. Rev. **49**, 16 248 (1994).
[21] C. Zener, Phys. Rev. **82**, 403 (1951).
[22] A. Urushibara, Y. Moritomo, T. Arima, A. Asamitsu, G. Kido, and Y. Tokura, Phys. Rev. B **51**, 14 103 (1995).
[23] See, e.g., G.D. Mahan, *Many-Particle Physics* (Plenum, New York, 1990), Chap. 6.
[24] Y. Yamada, O. Hino, S. Nohdo, R. Kanao, T. Inami, and S. Katano, Phys. Rev. Lett. **77**, 904 (1996).
[25] K. Wakamura, Solid State Commun. **71**, 1033 (1989).
[26] J.D. Lee and B.I. Min, Phys. Rev. B **55**, 12 454 (1997).
[27] H.Y. Hwang, S-W. Cheong, N.P. Ong, and B. Batlogg, Phys. Rev. Lett. **77**, 2041 (1996).
[28] G. Haacke and L.C. Beegle, Phys. Rev. Lett. **17**, 427 (1966).
[29] E.M. Kogan and M.I. Auslender, Phys. Status Solidi B **147**, 613 (1988).
[30] M. Robbins, H.W. Lehmann, and J.G. White, J. Phys. Chem. Solids **28**, 897 (1967).
[31] N.M. Kovtun, N.P. Neiden, V.K. Prokopenko, and A.A. Schemyakov, Zh. Éksp. Teor. Fiz. **77**, 404 (1979) [Sov. Phys. JETP **50**, 207 (1979)].
[32] S. Juszczyk and M. Gogolowicz, J. Magn. Magn. Mater. **92**, 388 (1991).
[33] F.K. Lotgering, R.P. Van Stapele, G.H.A.M. Van Der Steen, and J.S. Van Wieringen, J. Phys. Chem. Solids **30**, 799 (1969).
[34] G.Yu. Babaev, A.G. Kocharov, Kh. Ptasevich, I.I. Yamzin, M.A. Vinnik, Yu.G. Saksonov, V.A. Alferov, I.V. Gordeev, and Yu.D. Tret'yakov, Kristallografiya **20**, 550 (1975) [Sov. Phys. Crystallogr. **20-3**, 336 (1975)].
[35] E. Riedel, R. Karl, and R. Rackwitz, J. Solid State Chem. **40**, 255 (1981).